

The Interaction between CO and $\text{YBa}_2\text{Cu}_3\text{O}_x$ As Studied by TG/DTA, FTIR, and XPSJ. Lin,^{*†} K. G. Neoh,[†] N. Li,^{†‡} T. C. Tan,[†] A. T. S. Wee,[§] A. C. H. Huan,[§] and K. L. Tan[§]

Departments of Chemical Engineering and Physics, National University of Singapore, Singapore 0511

Received December 2, 1992

The interaction of CO with $\text{YBa}_2\text{Cu}_3\text{O}_x$ ($x \sim 7$) has been studied using differential thermal analysis (DTA)/thermogravimetry (TG), Fourier transform infrared spectroscopy (FTIR), and X-ray photoelectron spectroscopy (XPS). The interaction at temperatures between 400 and 800 K proceeds as $\text{CO} + \text{O}(\text{lattice}) = \text{CO}_2$, as shown by the evolved gas analysis and DTA/TG calorimetric measurement. At 800–1200 K a large CO uptake is observed, resulting in the formation of BaCO_3 , which is characterized by FTIR, and the reduction of Cu(II) and Y(III), as observed by XPS. An apparent activation energy of 16 kcal/mol and a heat of reaction of 60 kcal/mol are estimated for this high-temperature reaction from the DTA/TG studies. These results are compared with those obtained for $\text{YBa}_2\text{Cu}_3\text{O}_y$ ($y \sim 6$) and the composite compounds, CuO, Y_2O_3 , and BaCO_3 . A detailed mechanism which may explain the higher catalytic activity on $\text{YBa}_2\text{Cu}_3\text{O}_x$ than on CuO ³ is suggested.

Introduction

Cu-based oxides are presently the most widely used catalysts for methanol synthesis and the water-gas shift reaction.¹ They are also viewed as prospective catalysts for removing nitric oxide and carbon monoxide from automotive exhaust emissions.^{2,3} Recently, the well-known superconducting Y–Ba cuprates, including $\text{YBa}_2\text{Cu}_3\text{O}_7$, showed high catalytic activities,^{3–5} as well as strong affinity, toward some small-molecule gases, including O_2 , H_2 , H_2O , CO_2 , CO, and NO.^{5–10} In particular, the perovskite-type Y–Ba cuprates are found to be more active in catalyzing the reaction $\text{NO} + \text{CO} = \frac{1}{2}\text{N}_2 + \text{CO}_2$ than other types of copper catalysts.³ Therefore it is of practical significance to study the interaction between CO and the perovskite-type Y–Ba cuprates.

In this work two Y–Ba cuprates, $\text{YBa}_2\text{Cu}_3\text{O}_x$ and $\text{YBa}_2\text{Cu}_3\text{O}_y$, are prepared in the same way as reported in the literature, according to which $x \sim 7$ and $y \sim 6$.^{5,6} The interaction between CO and these samples is studied using simultaneous thermal analysis (STA), X-ray photoelectron spectroscopy (XPS), and Fourier transform infrared spectroscopy (FTIR). STA allows for the calorimetric measurement and kinetic study of the CO interaction by a combination of simultaneous differential thermal analysis (DTA), thermogravimetry (TG), and evolved gas analysis (EGA). FTIR is used to characterize the reaction products in the solid phase while XPS can provide information on changes in the oxidation states due to the reaction. The results obtained for the $\text{YBa}_2\text{Cu}_3\text{O}_x$ and $\text{YBa}_2\text{Cu}_3\text{O}_y$ samples are compared with

those for the composite compounds CuO, Y_2O_3 , and BaCO_3 . On the basis of these studies, a detailed mechanism of the interaction is postulated.

Experimental Section

The $\text{YBa}_2\text{Cu}_3\text{O}_x$ sample was prepared as described in the literature.⁵ Powder mixtures of Y_2O_3 (Fluka, AG), BaCO_3 (Merck, AG), and CuO (Fluka, AG) of the required stoichiometric ratio were pressed into pellets and calcined at 1200 K overnight in air. They were then reground well and repressed into pellets and sintered at 1200 K overnight again. The sample prepared was characterized on a JEOL JSM-T330A scanning electron microscope (SEM), with the atomic ratio of Y:Ba:Cu \approx 1:2:3 as determined by the energy-dispersive analysis of X-rays (EDAX). The value of x in $\text{YBa}_2\text{Cu}_3\text{O}_x$ thus prepared was reported to range from 6.5 to 6.9.⁵ The $\text{YBa}_2\text{Cu}_3\text{O}_y$ sample was obtained by heating the $\text{YBa}_2\text{Cu}_3\text{O}_x$ sample to 1200 K in N_2 . The TG measurement indicated that $\text{YBa}_2\text{Cu}_3\text{O}_y$ had \sim 1.4% weight loss, as compared with $\text{YBa}_2\text{Cu}_3\text{O}_x$. According to the literature, the weight loss was due to the removal of oxygen from the crystal,⁶ which would give a value close to 6 for y . The crystal structure of the $\text{YBa}_2\text{Cu}_3\text{O}_x$ sample was determined by powder X-ray diffraction (XRD), which was performed on a Philips PW1729 X-ray diffractometer with $\text{Cu K}\alpha$ radiation. The X-ray powder diffraction spectrum of the $\text{YBa}_2\text{Cu}_3\text{O}_x$ sample was found to be identical to those reported in the literature, indicating that the sample prepared was indeed a single phase with the known perovskite-type structure.^{5,6}

The simultaneous thermal analysis was performed on a Netzsch STA 409. Approximately 100–200 mg of the sample prepared as described above was placed in an open crucible and heated from room temperature to \sim 1200 K at a linear rate of 10 °C/min by a temperature-programmed heater. The same amount of kaolin, a thermally and chemically inert material, was loaded in another identical and symmetrically located crucible as the reference. Two thermocouples attached to the crucibles measured the temperature dependence (ΔT) between the sample and the reference material, providing information on the heat flow during the experiment. CO was passed through the sample at a flow rate of 100 mL/min for studying its interaction with the sample. The temperature difference (ΔT) was continuously recorded as a function of temperature, giving the differential thermal analysis (DTA) curve, while the weight of the sample was recorded as a thermogravimetry (TG) plot. For a quantitative evaluation of the DTA signals, calibration was performed by melting standard materials such as Sn or K_2CrO_4 . The calibration factor was determined by the calculation of the quotient of the real heat of melting of the standard materials and the area of the DTA peak. The weight change during the reaction was determined on the basis of the departure of the TG curve from the baseline. The evolved gas was analyzed by gas chromatography (GC) on a Shimadzu GC-14A using a Poropak Q (2 m long) column with helium gas as the carrier gas (30 mL/min).

The infrared spectra of the samples were recorded on a Shimadzu FTIR-8101 using the pellet technique, which involved mixing the finely ground sample with potassium bromide powder and pressing the mixture

[†] Department of Chemical Engineering.

[‡] Present address: Department of Minerals Engineering and Extractive Metallurgy, Western Australian School of Mines, P.O. Box 597, Kalgoorlie 6430, Western Australia, Australia.

[§] Department of Physics.

- (1) Bridger, G. W.; Spencer, M. S. In *Catalyst Handbook*, 2nd ed.; Twigg, M. V., Ed.; Wolfe Publishing Ltd.: London, 1989; p 446 and references therein.
- (2) Ross, J. *Appl. Catal.* **1992**, *B1*, N18 and references therein.
- (3) Halasz, I.; Brenner, A.; Shelef, M.; Ng, K. Y. S. *Catal. Lett.* **1991**, *11*, 327 and references therein.
- (4) Hansen, S.; Otamiri, J.; Bovin, J.; Anderson, A. *Nature* **1988**, *334*, 143.
- (5) Mizuno, N.; Yamato, M.; Misono, M. *J. Chem. Soc., Chem. Commun.* **1988**, 887.
- (6) Gallagher, P. K.; O'Bryan, H. M.; Sunshine, S. A.; Murphy, D. W. *Mater. Res. Bull.* **1987**, *22*, 995.
- (7) Haller, I.; Shafer, M. W.; Figat, R.; Goland, D. B. In *Chemistry of Oxide Superconductors*; Rao, C. N. R., Ed.; Blackwell Scientific Publications: London, 1988; p 93.
- (8) Yan, M. F.; Barn, R. L.; O'Bryan, H. M.; Gallagher, P. K.; Sherwood, R. C.; Jin, S. *Appl. Phys. Lett.* **1987**, *51*, 532.
- (9) Qiu, S. L.; Ruckman, M. W.; Brookes, N. B.; Johnson, D.; Chen, J.; Lin, C. L.; Strongin, M.; Sinkovic, B.; Crow, J. E.; Jee, C. *Phys. Rev. B* **1988**, *37*, 3747.
- (10) McCallum, R. W. *J. Met.* **1989**, 50.

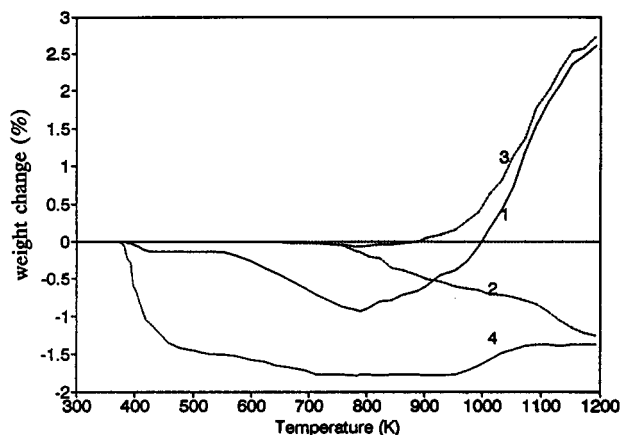


Figure 1. TG data with a linear heating rate of 10 °C/min for (1) $\text{YBa}_2\text{Cu}_3\text{O}_x$ in CO, (2) $\text{YBa}_2\text{Cu}_3\text{O}_x$ in N_2 , (3) $\text{YBa}_2\text{Cu}_3\text{O}_y$ in CO, and (4) CuO in CO. Weight change (%) is determined by the quotient of the weight change, ΔW , and the initial weight of the sample, W .

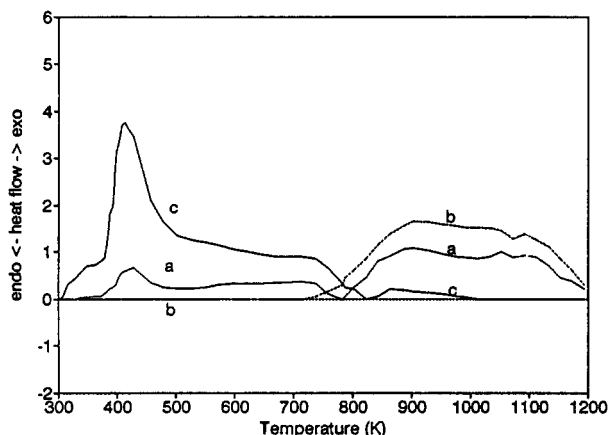


Figure 2. DTA data with a linear heating rate of 10 °C/min for (a) $\text{YBa}_2\text{Cu}_3\text{O}_x$ in CO, (b) $\text{YBa}_2\text{Cu}_3\text{O}_y$ in CO, and (c) CuO in CO. Heat flow is determined by the measurement of the differential temperature (ΔT) in mV/unit.

in an evacuable die at 8 tons of pressure to produce a transparent disk. Forty scans were taken for each spectrum to obtain a good signal-to-noise ratio.

The XPS experiments were performed on a VG ESCALAB MKII spectrometer using a Mg $K\alpha$ X-ray source (1253.6 eV, 120 W) at a constant analyzer pass energy of 20 eV. With an ultimate base pressure of $\sim 5 \times 10^{-10}$ mbar, the normal operating pressure in the analysis chamber was $< 2 \times 10^{-9}$ mbar during the course of the measurements.

Results and Analysis

1. CO Interaction at Temperatures below 800 K. The differential thermal analysis (DTA) and thermogravimetry (TG) results for the interaction of CO with $\text{YBa}_2\text{Cu}_3\text{O}_x$, $\text{YBa}_2\text{Cu}_3\text{O}_y$, and their composite compounds are illustrated in Figures 1 and 2, respectively. Curve 1 in Figure 1 is the TG data for the $\text{YBa}_2\text{Cu}_3\text{O}_x$ sample which was heated to 1200 K in CO in the Netzsch STA 409. Curve 2 in Figure 1 was obtained by heating the $\text{YBa}_2\text{Cu}_3\text{O}_x$ sample under N_2 in the STA 409, which resulted in the formation of $\text{YBa}_2\text{Cu}_3\text{O}_y$. After cooling to room temperature, the $\text{YBa}_2\text{Cu}_3\text{O}_y$ sample was heated to 1200 K in CO at a linear rate of 10 °C/min, giving curve 3. The composite compounds CuO, Y_2O_3 , and BaCO_3 were also studied by STA. CuO reacts with CO strongly as shown in curve 4 of Figure 1. The data for the Y_2O_3 and BaCO_3 samples are not presented, since little change in the sample weight was observed for the Y_2O_3 and BaCO_3 samples heated in CO, even if they were pretreated, prior to the interaction with CO, by the same procedure as in the preparation of the $\text{YBa}_2\text{Cu}_3\text{O}_x$ sample. This indicates that these two composite compounds of $\text{YBa}_2\text{Cu}_3\text{O}_x$ are fairly stable with respect to heating

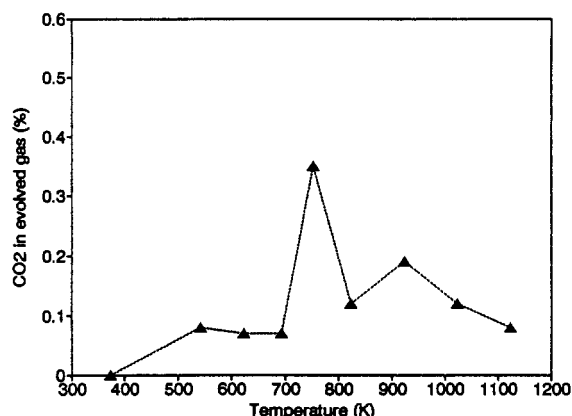
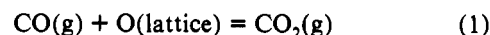


Figure 3. Evolved CO_2 analysis by GC for the $\text{YBa}_2\text{Cu}_3\text{O}_x$ sample heated (at 10 °C/min) in CO (with a flow rate of 100 mL/min).

and CO interaction at temperatures below 1200 K. The DTA results are illustrated in Figure 2 with curves a–c referring to the $\text{YBa}_2\text{Cu}_3\text{O}_x$, $\text{YBa}_2\text{Cu}_3\text{O}_y$, and CuO samples heated in CO at a linear rate of 10 °C/min, respectively. As shown in curve 1 of Figure 1 and curve a of Figure 2, $\text{YBa}_2\text{Cu}_3\text{O}_x$ has exhibited simultaneous weight loss ($\sim 1\%$) and heat release at temperatures between 400 and 800 K. The evolved gas analysis (EGA) by GC indicates that CO_2 is the unique product in the evolved gas and its concentration has a maximum at temperatures between 700 and 800 K (see Figure 3). The EGA results are in a good agreement with the TG data shown in curve 1 of Figure 1, leading to the conclusion that the loss in the sample weight under these conditions is totally due to the formation and evolution of CO_2 . Thus the interaction between CO and $\text{YBa}_2\text{Cu}_3\text{O}_x$ at 400–800 K can be expressed as

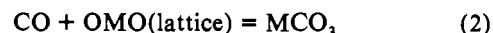


On the basis of this observation, a quantitative evaluation of the thermal effect of the reaction can be performed. A reaction heat, ΔH , of 38 kcal/mol is derived from the DTA/TG results according to the following formula:

$$\Delta H = Q/(\Delta W/16)$$

where Q is the heat release measured from the DTA study and ΔW the weight loss (due to the depletion of the lattice oxygen as shown in reaction 1) obtained from the TG curve. This value is almost the same as that reported in the literature,¹¹ giving weight to the conclusion derived from the EGA study. No evident interaction is observed between CO and $\text{YBa}_2\text{Cu}_3\text{O}_y$ in this temperature region (see curve 3 in Figure 1 and curve b in Figure 2). As shown in curve 4 of Figure 1 and curve c of Figure 2, CuO reacts strongly with CO in this temperature range. The EGA and calorimetric measurements of the heat of reaction give results very similar to those observed for the $\text{YBa}_2\text{Cu}_3\text{O}_x$ sample.

2. CO Interaction at High Temperatures (800–1200 K). Further enhancement in the reaction temperature for the CO/ $\text{YBa}_2\text{Cu}_3\text{O}_x$ system results in the rapid increase in the weight of the $\text{YBa}_2\text{Cu}_3\text{O}_x$ sample and in the simultaneous strong heat release (see curve 1 of Figure 1 and curve a of Figure 2). The exothermic heat effect measured corresponds to a heat of reaction of 60 kcal/mol, if it is postulated that the increase in the weight is due to the uptake of CO through the reaction



The heat of reaction thus measured agrees well with the known value reported in the literature,¹¹ supporting the above assumption. The formation of the carbonate in the solid phase as the result of the CO interaction has been confirmed by the FTIR study. In

(11) Stone, F. S. *Adv. Catal.* **1962**, *13*, 1.

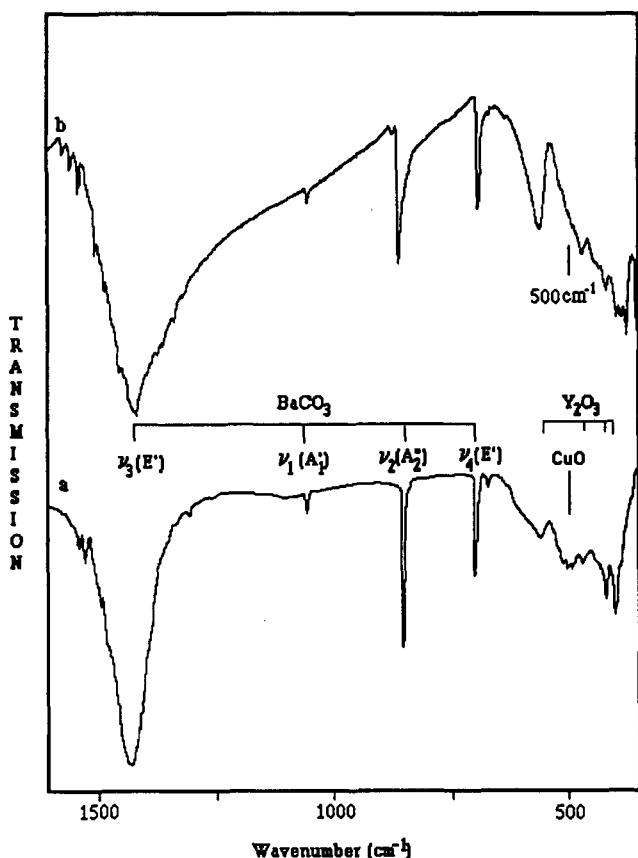


Figure 4. Comparison of the FTIR spectra obtained from (a) a mixture of BaCO₃, Y₂O₃, and CuO and (b) the YBa₂Cu₃O_x sample after interaction with CO at temperatures up to 1200 K.

Figure 4 the infrared spectra are displayed for a mixture of BaCO₃, Y₂O₃, and CuO (spectrum a) and for the YBa₂Cu₃O_x sample after the interaction with CO at high temperatures (spectrum b). In the wavenumber region between 650 and 1600 cm⁻¹ the two spectra are basically the same. This is strong evidence of the formation of BaCO₃ resulting from the CO interaction, since, according to the literature¹² as well as our FTIR results on pure BaCO₃, the absorption bands at 1420, 1060, 855, and 695 cm⁻¹ are due to BaCO₃ with the aragonite structure and can be assigned to ν₃(E'), ν₁(A₁'), ν₂(A₂'), and ν₄(E') for the CO₃ group. In the lower wavenumber region (350–650 cm⁻¹) the infrared bands at 500 cm⁻¹, which are found in spectrum a but not in spectrum b, are due to the Cu(II)–O stretching vibrations, while the bands at 560, 420, and 400 cm⁻¹, which are observed in both spectrum a and spectrum b, are due to yttrium oxides, on the basis of experiments on pure CuO and Y₂O₃. The similarity between spectra a and b in the bands due to yttrium oxides appears to indicate that, in addition to barium carbonate, yttrium oxide may also be a product of the CO interaction of YBa₂Cu₃O_x. On the other hand, the fact that no evident signals are observed in spectrum b at 500 and 620 cm⁻¹, where the Cu–O stretching vibration is normally observed with the presence of pure CuO (500 cm⁻¹) or Cu₂O (620 cm⁻¹), seems to mean that copper oxides may not be the products of the CO interaction of YBa₂Cu₃O_x. This conclusion is in a good agreement with the XPS results, which show that most of the Cu atoms in the crystal are reduced to Cu(0) after the CO interaction (vide infra).

It is possible to evaluate the activation energy of the reaction from the TG data.¹³ In reaction 2 the concentration of CO can be regarded as a constant (e.g. 1) so that the reaction rate appears

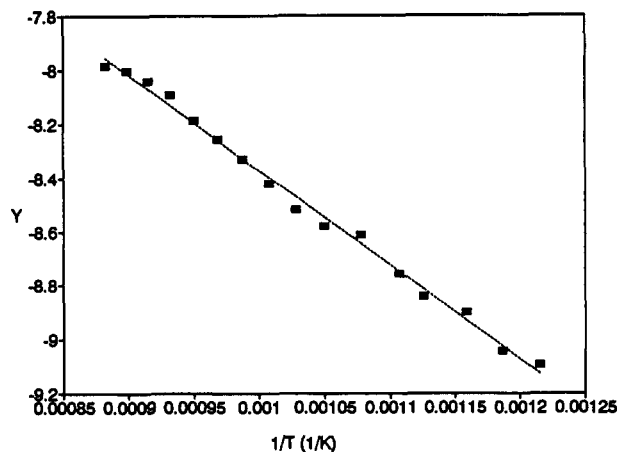


Figure 5. $Y-1/T$ plot based on the TG data obtained from curve 1 in Figure 1 (for CO/YBa₂Cu₃O_x at the temperatures above 800 K). $Y = \log\{-\log(1-M)/T^2\}$, where M is the weight change for the sample at temperature T as compared with that at 800 K. The slope of the straight line is equal to $-E/2.3R$, which gives the apparent activation energy, E , of 16 kcal/mol.

to depend only on the concentration of the active sites in the solid phase and may be expressed by

$$dM/dt = k(1-M)^n \quad (3)$$

where M is the fraction of the active sites in the sample, which have been bound to CO. Obviously, M corresponds to the increase in the sample weight. In eq 3, n is the order of reaction and may be reasonably assumed to equal 1 in this case, while k is the reaction constant given by the expression

$$k = A \exp(-E/RT) \quad (4)$$

where A denotes the frequency factor and E the activation energy.

By rearrangement and integration of eqs 3 and 4, the following equation can be derived:¹³

$$\log\{-\log_{10}(1-M)/T^2\} = \log\{(AR/ae)[1 - (2RT/E)]\} - E/(2.3RT) \quad (5)$$

where $a = dT/dt$ is the linear heating rate in °C/min. Thus a plot of Y ($Y = \log\{-\log(1-M)/T^2\}$) versus $1/T$ should result in a straight line with the slope equal to $-E/2.3R$ if the above postulations are correct. The results obtained on the basis of the data for curve 1 in Figure 1 are displayed in Figure 5. The good linear fit of the plot in the temperature region between 900 and 1100 K seems to confirm that the reaction is first order with respect to the active-site number as postulated. The slope of the straight line gives $E = 16$ kcal/mol.

In the high-temperature region, the DTA/TG and FTIR results for YBa₂Cu₃O_y are similar to those for YBa₂Cu₃O_x, indicating a similar reaction is taking place. On the other hand, as shown in Figures 1 and 2, CuO does not react with CO to a significant extent in this temperature region.

Figures 6–8 illustrate the Cu 2p_{3/2}, Cu LVV, and Y 3d spectra, respectively, for the YBa₂Cu₃O_x and YBa₂Cu₃O_y samples before and after the interaction with CO at elevated temperatures (up to 1200 K). Many changes are observed in these XPS spectra due to the interaction of CO. As shown in spectrum a of Figure 6, YBa₂Cu₃O_x has its Cu 2p_{3/2} peak located at the binding energy of 933.4 eV, with a strong satellite at 942.3 eV, indicating that the Cu atoms in the YBa₂Cu₃O_x sample exist mainly in the Cu(II) oxidation state before the interaction with CO. After the interaction with CO, the width of the Cu 2p_{3/2} peak is found to increase, with most of the Cu 2p_{3/2} intensity shifted to lower binding energy by 1.6 eV, and the satellite intensity is shown to reduce greatly (see spectrum b in Figure 6). This appears to mean that most of the Cu atoms in YBa₂Cu₃O_x have been reduced by CO (species ii in spectrum b of Figure 6) although some (species

(12) Nakamoto, K. In *Infrared and Raman Spectra of Inorganic and Coordination Compounds*, 4th ed.; John Wiley & Sons: New York, 1986; see also references therein.

(13) Coats, A. W.; Redfern, J. P. *Nature* 1964, 201, 68.

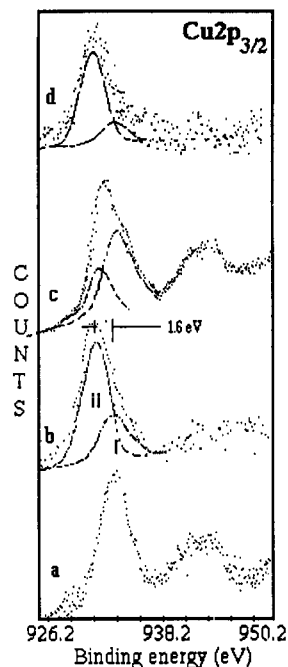


Figure 6. Comparison of the Cu $2p_{3/2}$ X-ray photoelectron spectra obtained from (a) the $\text{YBa}_2\text{Cu}_3\text{O}_x$ sample before the CO interaction, (b) the $\text{YBa}_2\text{Cu}_3\text{O}_x$ sample after the CO interaction, (c) the $\text{YBa}_2\text{Cu}_3\text{O}_y$ sample before the CO interaction, and (d) the $\text{YBa}_2\text{Cu}_3\text{O}_y$ sample after the CO interaction. The spectra were recorded by using a Mg $K\alpha$ X-ray source (1253.6 eV, 120 W) at a constant analyzer pass energy of 50 eV. The charging shifts of the samples have been corrected by using the binding energy of the contaminant C 1s = 284.6 eV below the Fermi level as reference. The peaks of broken lines were produced by a peak-synthesis procedure that fixed the peak positions and widths and varied the heights to achieve a best fit of the experimental (dotted) spectra. i and ii denote the copper species with different oxidation states.

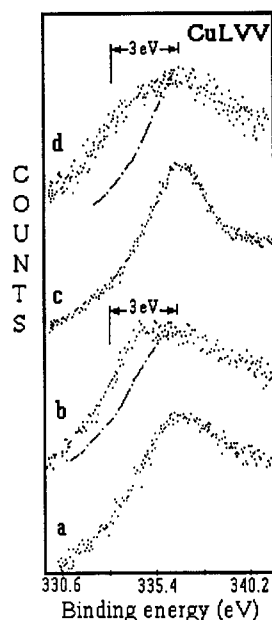


Figure 7. Comparison of the Cu LVV Auger spectra obtained from (a) the $\text{YBa}_2\text{Cu}_3\text{O}_x$ sample before the CO interaction, (b) the $\text{YBa}_2\text{Cu}_3\text{O}_x$ sample after the CO interaction, (c) the $\text{YBa}_2\text{Cu}_3\text{O}_y$ sample before the CO interaction, and (d) the $\text{YBa}_2\text{Cu}_3\text{O}_y$ sample after the CO interaction. The spectra were obtained under the same conditions as for Figure 6. Broken lines are shown in spectra b and d for convenient comparison of spectra a with b and spectra c with d.

i) still retain the high oxidation state. In order to determine whether the reduction product (species ii) is Cu(0) or Cu(I), it is necessary to measure the Auger parameter,¹⁴ since Cu(I) and Cu(0) are known to have the same binding energy for their Cu

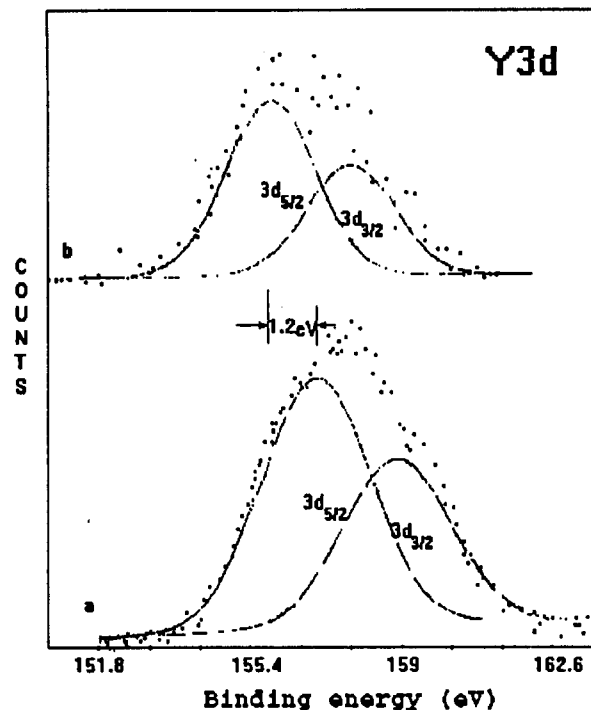


Figure 8. Comparison of the Y 3d spectra obtained from (a) the $\text{YBa}_2\text{Cu}_3\text{O}_x$ sample before the CO interaction and (b) the $\text{YBa}_2\text{Cu}_3\text{O}_x$ sample after the CO interaction under the same conditions as for Figure 6. The peaks of the broken lines were obtained for the $3d_{5/2}$ and $3d_{3/2}$ components by the same peak-synthesis procedure as in Figure 6.

$2p$ peaks but different values for their Auger Cu LVV peaks. By comparison of Auger spectra a and b in Figure 7, the interaction of CO with $\text{YBa}_2\text{Cu}_3\text{O}_x$ is found to result in the shift of some of the Auger electron intensity to lower binding energy by about 3 eV. This gives an Auger parameter of 1851 eV for the CO-reduced copper species (species ii in Figure 6), indicating that most of the copper atoms in the $\text{YBa}_2\text{Cu}_3\text{O}_x$ sample are reduced to Cu(0) after the CO interaction. Spectra a and b in Figure 8 represent the Y 3d peaks obtained for the $\text{YBa}_2\text{Cu}_3\text{O}_x$ samples before and after the interaction with CO. Obviously the Y 3d peaks are shifted to lower binding energy by 1.2 eV due to the CO interaction, indicating that the yttrium atoms in $\text{YBa}_2\text{Cu}_3\text{O}_x$ have been reduced by CO. Little change is observed in the Ba 3d spectrum for the $\text{YBa}_2\text{Cu}_3\text{O}_x$ sample upon the CO interaction.

Spectrum c in Figure 6 is obtained from the $\text{YBa}_2\text{Cu}_3\text{O}_y$ sample before the interaction with CO. A comparison of spectra c and a shows that when $\text{YBa}_2\text{Cu}_3\text{O}_x$ is heated in N_2 , about one-third of the Cu $2p_{3/2}$ intensity shifts to lower binding energy by 1.6 eV. On the other hand, in comparison with spectrum a in Figure 7, the Auger spectrum of the $\text{YBa}_2\text{Cu}_3\text{O}_y$ sample (spectrum c in Figure 7) is found to peak in the same energy region, but with less intensity in the higher binding energy region. These are characteristic of Cu(I).¹⁵ This indicates that heating $\text{YBa}_2\text{Cu}_3\text{O}_x$ in N_2 at elevated temperatures would result in the reduction of some Cu(II) to Cu(I) because of the removal of oxygen as reported in the literature.¹⁶ Spectrum d in Figure 6 is the Cu $2p_{3/2}$ spectrum recorded for the $\text{YBa}_2\text{Cu}_3\text{O}_y$ sample after the interaction with CO. In comparison with spectrum c in Figure 6, more intensity is shifted to lower binding energy in spectrum d, showing that the CO interaction results in the further reduction of the Cu(II)

- (14) Wagner, C. D.; Riggs, W. M.; Davis, L. E.; Moulder, J. F.; Mullenberg, G. E. In *Handbook of X-ray Photoelectron Spectroscopy*; Perkin-Elmer: Eden Prairie, MN, 1979.
- (15) Ramaker, D. E.; Tuener, N. H.; Murday, J. S.; Toth, L. E.; Osofsky, M.; Hutson, F. L. *Phys. Rev. B* 1987, 36, 5672.
- (16) Goodenough, J. B.; Manthiram, A. In *Chemistry of Oxide Superconductors*; Rao, C. N. R., Ed.; Blackwell Scientific Publications: London, 1988; p 101.

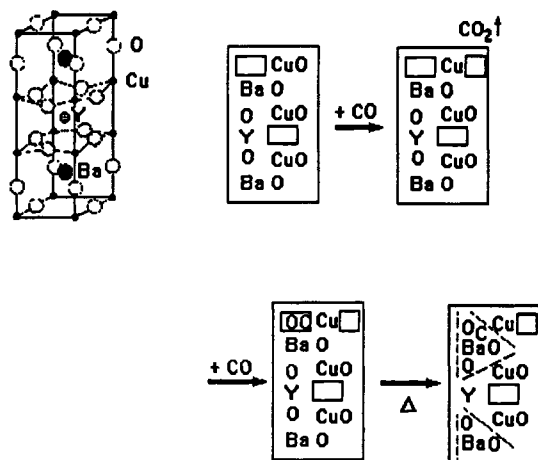


Figure 9. Schematically illustrated mechanism for the interaction of CO with the $\text{YBa}_2\text{Cu}_3\text{O}_x$ sample. The crystal structure to the left is the unit cell of the perovskite-type structure for the $\text{YBa}_2\text{Cu}_3\text{O}_x$ sample with $x = 6.5-6.9$.^{5,17} The blocks represent the unit cells during the interaction with CO at elevated temperatures.

species in the $\text{YBa}_2\text{Cu}_3\text{O}_x$ sample. Comparing spectra c and d in Figure 7 shows that the reduced copper species exists mostly in the Cu(0) state, in analogy with the CO/ $\text{YBa}_2\text{Cu}_3\text{O}_x$ case. The Y 3d spectra for the $\text{YBa}_2\text{Cu}_3\text{O}_x$ sample before and after the CO interaction are very similar to spectra a and b in Figure 8, indicating that Y(III) in $\text{YBa}_2\text{Cu}_3\text{O}_x$ is also reduced by CO. No change in the Ba 3d spectrum is found after the interaction of $\text{YBa}_2\text{Cu}_3\text{O}_x$ with CO.

Discussion

In summary, the evolved gas analysis and the calorimetric measurements in the DTA/TG studies have shown that at 400–800 K CO reacts with the $\text{YBa}_2\text{Cu}_3\text{O}_x$ sample, forming $\text{CO}_2(\text{g})$ with the exothermic heat flow corresponding to 38 kcal/mol. At higher temperatures (up to 1200 K) the uptake of large amounts of CO is observed by TG, resulting in the formation of BaCO_3 , which is characterized by FTIR, as well as the reduction of Y(III) and Cu(II), as detected by XPS. This high-temperature interaction is a first-order reaction, with an apparent activation energy of 16 kcal/mol and a heat of reaction of 60 kcal/mol, as estimated from the DTA/TG studies. The oxygen-deficient sample, $\text{YBa}_2\text{Cu}_3\text{O}_y$, does not react with CO at the temperatures below 800 K but shows behavior similar to that of the $\text{YBa}_2\text{Cu}_3\text{O}_x$ sample at 800–1200 K. CuO reacts significantly with CO mainly at 400–800 K. Evidently, neither BaCO_3 nor Y_2O_3 reacts with CO in the entire temperature region studied.

On the basis of the above experimental results and the knowledge available in the literature concerning the crystal structures of Y–Ba cuprates, it is possible to discuss the mechanism of the CO interaction and its catalytic applications. The $\text{YBa}_2\text{Cu}_3\text{O}_x$ sample prepared as described in the Experimental Section has been reported to have a perovskite-type crystal structure,^{5,17} which contains in each unit cell one CuO plane, two BaO planes, two CuO_2 planes, and one Y plane stacked in the following sequence: CuO/BaO/ CuO_2 /Y/ CuO_2 /BaO, (see Figure 9). All the oxygen atoms in the crystal assume perovskite-like anion positions, halfway between Cu atoms along cube edges. Nevertheless not all the anion positions are occupied: the anion positions in the CuO plane are only half-occupied and may be ordered to form a CuO chain, while all the anion positions in the yttrium plane are vacant so that the oxygen atoms in the CuO_2 planes which are next to the yttrium plane are slightly displaced

toward yttrium. It is well established that the oxygen atoms in the CuO_2 planes are strongly bound and cannot be removed without phase decomposition, while the oxygen atoms in the CuO chains are loosely bound and can be easily removed.^{16,17} Therefore heating $\text{YBa}_2\text{Cu}_3\text{O}_x$ in N_2 above 700 K easily removes the oxygen atoms in the CuO planes, resulting in the weight loss (as observed from curve 2 in Figure 1) and the formation of the oxygen-deficient sample, $\text{YBa}_2\text{Cu}_3\text{O}_y$. In the presence of CO, the removal of the oxygen atoms becomes even easier and can occur at much lower temperatures (400–800 K) (as shown in curve 1, Figure 1). This low-temperature interaction results in the formation and evolution of CO_2 with the creation of new oxygen vacancies in the CuO plane (as schematically illustrated in block 2 in Figure 9). In the $\text{YBa}_2\text{Cu}_3\text{O}_y$ sample most of the loosely bound oxygen atoms have been removed upon heating so that not evident reaction with CO was observed at temperatures below 800 K. Note that the DTA/TG results observed for the CO interaction with the $\text{YBa}_2\text{Cu}_3\text{O}_x$ sample at 400–800 K are very similar to those for CuO. It appears that the reaction $\text{CO} + \text{O}(\text{lattice}) = \text{CO}_2$ occurring on $\text{YBa}_2\text{Cu}_3\text{O}_x$ may follow a mechanism somewhat similar to that which has been suggested for CO adsorption on transition metal oxides such as MnO_2 , CuO, and NiO.^{11,18,19} According to this mechanism, the general adsorbed state of CO on an oxide surface is the surface carbonate, which may then decompose or react with CO, forming CO_2 .

Previous studies using EXAFS, Mössbauer spectroscopy, and other structure-sensitive methods have shown that the interaction of halogen with $\text{YBa}_2\text{Cu}_3\text{O}_x$ proceeds by intercalation of halogen into the vacant anion positions in the CuO layers of the $\text{YBa}_2\text{Cu}_3\text{O}_x$ structure.²⁰ In the present study the removal of the oxygen atoms from the unit cell of $\text{YBa}_2\text{Cu}_3\text{O}_x$ by CO at the temperatures of 400–800 K appears to result in breaking certain interionic bonds, softening the structure, and creating more oxygen vacancies in the CuO chains. These oxygen vacancies may serve as the active centers for the CO intercalation. The intercalated $\text{YBa}_2\text{Cu}_3\text{O}_x$ appears to be a metastable compound and can undergo chemical transformation at elevated temperatures, leading to the degradation of the matrix and to the formation of more thermodynamically stable products. Note that the BaO layer falls between the CuO_2 and the CuO planes so that the Ba atoms may share its coordinated oxygen atoms as well as oxygen vacancies with the copper atoms in the CuO planes. In other words the Ba atoms are in the nearest positions to the intercalated CO ($<3 \text{ \AA}$, according to the known structure¹⁹) (see block 3 in Figure 9). Since BaCO_3 is thermodynamically more stable than CuCO_3 , which does not exist in nature and has never been produced in laboratories, the CO interaction may appear to proceed with the eventual formation of BaCO_3 , rather than CuCO_3 , as observed from the FTIR and XPS studies. Since CO is a strong electron acceptor, it should be expected that the interaction between CO and $\text{YBa}_2\text{Cu}_3\text{O}_x$ is a redox reaction which involves an electron transfer from Cu(II) to the intercalated CO. The oxygen atoms in the CuO_2 planes are also coordinated to the Ba atoms according to the known structure (see Figure 9) so that the formation of BaCO_3 would eventually reduce the number of the oxygen atoms coordinated to the Cu(II) atoms, leading to a reduction in the oxidation state of the Cu atoms, which is observed in this study by XPS. Similarly, the formation of BaCO_3 would also change the environment of the Y(III) atoms which share their near-neighbor oxygen atoms with Ba(II). As a result, the near-neighbor oxygen atoms of Y, which are originally displaced toward Y, may move toward Ba, leading to the partial reduction of the Y(III) atoms, as observed from the XPS study. This mechanism is schematically illustrated in Figure 9.

(18) Katz, M. *Adv. Catal.* **1953**, *5*, 177.

(19) Bielski, A.; Haber, J. In *Oxygen in Catalysis*; Marcel Dekker: New York, 1991; Chapter 6.

(20) Nemudry, A. P.; Pavlukhin, Y. T.; Hainovsky, N. G.; Boldyrev, V. V. *J. Solid State Chem.* **1991**, *93*, 1.

(17) Hazen, R. M. In *Physical Properties of High Temperature Superconductors II*; Ginsberg, D. M., Ed.; World Scientific: Singapore, 1990; p 121.

The above-postulated mechanism has shown the important role that the perovskite structure may play in CO uptake by Y-Ba cuprates: it can offer the mobility of oxygen ions, favoring the oxidation of adsorbed molecules with the creation of active centers for further CO uptake; it can offer structure stabilizers such as Ba(II) ions, which are well distributed at coordination sites nearest to the active centers, aiding the absorption of CO through the formation of carbonate. Surface carbonate has been suggested to be an important intermediate in the oxidation reaction of CO over transition oxides.^{11,18,19} Therefore the earlier observations of the higher catalytic activity for the reaction $\text{CO} + \text{NO} = \frac{1}{2}\text{N}_2 + \text{CO}_2$ on the perovskite-type barium cuprates than on CuO and other non-perovskite Cu-containing catalysts may become understandable.³ In addition, the perovskite-type structure of yttrium-barium cuprates has shown an ability to retain some copper atoms in high oxidation states even under vigorous reduction conditions (in the presence of CO at high temperatures). This may be significantly important for the

methanol synthesis from syngas over copper-based catalysts since copper atoms in higher oxidation states may play a different role in CO activation compared to the metallic copper atoms.^{21,22} Furthermore, from the SEM X-ray map studies we also observed the stabilization of active metals including Cu, Ba, and Y in high dispersion against the CO interaction at elevated temperatures. All of these are valuable properties for catalysis and therefore offer the perovskite-type yttrium-barium cuprates the potential to serve as good catalysts for CO reactions.

Acknowledgment. We thank Mr. S. K. Tung for his valuable assistance in the SEM study and Mrs. S. W. Phua and T. J. Pang for their assistance in the XRD measurements.

-
- (21) Didziulis, S. V.; Butcher, K. D.; Cohen, S. L.; Solomon, E. I. *J. Am. Chem. Soc.* **1989**, *111*, 7110.
(22) Lin, L.; Jones, P.; Guckert, J.; Solomon, E. I. *J. Am. Chem. Soc.* **1991**, *113*, 8312.